ChemComm

COMMUNICATION

View Article Online
View Journal | View Issue

Cite this: *Chem. Commun.*, 2020, **56**, 3757

Received 7th January 2020,
Accepted 25th February 2020

DOI: 10.1039/d0cc00155d

rsc.li/chemcomm

Polymyxin-based photosensitizer for the potent and selective killing of Gram-negative bacteria†

Muhammed Ucuncu,‡[a] Bethany Mills,‡[b] Sheelagh Duncan,[b] Matteo Staderini,[a] Kevin Dhaliwal[b] and Mark Bradley *[a]

Here we report the synthesis of a novel methylene blue-polymyxin conjugate and demonstrate its light-mediated killing of Gram-negative bacteria on skin models of infection demonstrating a 10^8 decrease in bacterial colony-forming units.

Infectious diseases are one of the leading causes of morbidity and mortality globally[1,2] and during the 20th century, major advances in the discovery and development of antibiotics led to improved survival from bacterial infections.[3] However, overuse, misuse and environmental factors have led to a global increase in antimicrobial resistance (AMR). As such the development of new treatment strategies are imperative to combat the rise in antimicrobial resistance and to help sustain modern medical practice, with the pivotal need to develop strategies that cannot give rise to resistance.[4,5]

Photodynamic therapy (PDT) is widely utilised for the treatment of solid tumours, psoriasis, a variety of dental applications and surface decontamination.[6–10] PDT utilizes a photosensitizer (PS) which is activated by light to produce highly reactive oxygen species (ROS), including hydroxyl radicals (Type I photo-process) and singlet oxygen (Type II photo-process).[11]

However, the potential scope of PDT extends to a broad spectrum of targets, including pathogens (bacteria, fungi and viruses), where its mode of action would be unlikely to give rise to resistance.[12–14] Thus over the last two decades, photodynamic inactivation strategies to kill bacteria have been investigated,[13–15] however they have often suffered from poor selectivity and antimicrobial PDT has not been widely adopted in the clinic in large part due to the lack of bacterial targeting photo-sensitising agents.[14,16–18] Several attempts to improve the selectivity and sensitivity of antimicrobial PDT have been reported. The most common approaches have involved co-application of a PS together with a membrane disorganising agent or with the PS covalently coupled to a targeting unit.[19–23] However, studies have typically explored antimicrobial PDT against planktonic bacteria, rather than those within more clinically relevant infections.[14,24] This is important as in biofilms bacteria are located within an extracellular polymer matrix, where there is often poor drug penetration and reduced killing efficacy, with the minimum biofilm eradication concentration of the antimicrobial agent often 100-fold higher than the standard minimum inhibitory concentration.[25] Thus the aim of this study was to design, synthesise and validate a novel antimicrobial PDT agent that exhibits high selectivity and sensitivity against Gram-negative bacteria, including those within biofilms.

In the design of our Gram-negative antimicrobial PDT agent, we utilised polymyxin B that had been modified to remove its hydrophobic tail and adapted with a photosensitizer that would give high killing efficiency while offering low dark toxicity (Scheme 1). Polymyxin B (PMX-B) is a non-ribosomal cyclic lipopeptide antibiotic, increasingly utilised to treat Gram-negative bacterial infections. The mechanism of action is dual fold and is based on the electrostatic interaction of the protonated γ-amino units in the cyclic heptapeptide with the negatively charged lipopolysaccharides of the bacterial outer membrane and anchoring of the hydrophobic fatty acid tail and the D-Phe and L-Leu units through insertion into the outer membrane. This bivalent, entropically driven binding disrupts cell membrane integrity and results in cell lysis.[26] Previously, Nitzan *et al.* showed the synergistic effect of polymyxin on antimicrobial photodynamic therapy[27] while Guern used a polymyxin B scaffold as a targeting unit.[28,29] In their study, a cationic porphyrin (as the photosensitizer) was coupled to polymyxin B *via* thiol maleimide chemistry, however their probe lost specificity and killed both Gram-positive and negative bacteria, perhaps due to the fact that thiol maleimide chemistry is reversible or the non-selective nature of cationic porphyrins to bacteria. In our antimicrobial

[a] *School of Chemistry and the EPSRC IRC Proteus, University of Edinburgh, Joseph Black Building, David Brewster Road, Edinburgh, EH9 3FJ, UK. E-mail: mark.bradley@ed.ac.uk*
[b] *EPSRC Proteus Hub, Centre of Inflammation Research, Queen's Medical Research Institute, University of Edinburgh, 47 Little France Crescent, EH16 4TJ, Edinburgh, UK*

† Electronic supplementary information (ESI) available: Chemistry and biology methods and characterization data. See DOI: 10.1039/d0cc00155d

‡ Authors contributed equally to the work.

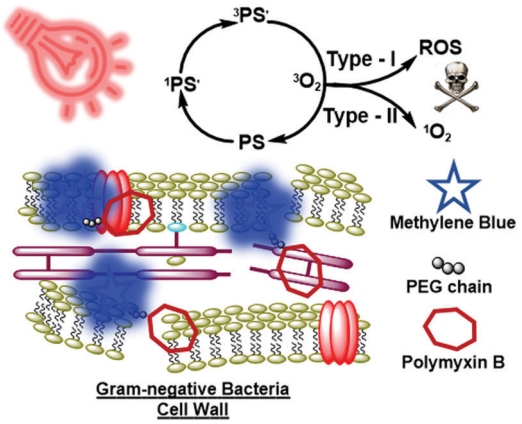

Scheme 1 Mode of action of the bacterial targeting antimicrobial photodynamic therapy agent MB-PMX.

PDT agent design we selected methylene blue (MB) which is an FDA approved photosensitizer with high photo-stability and red shifted absorbance (providing slighter deeper light penetration), while having high singlet oxygen (and other reactive oxygen species) quantum yields.[30]

Probe synthesis began by removing the hydrophobic tail of PMX-B using papain.[31] The side chains of the five L-diaminobutyric acid residues were protected using Boc-ON[31] allowing selective amide coupling chemistry to attach both a small polyethylene glycol spacer (using Fmoc-NH-$(EG)_2$-CH_2-COOH using DIC) and methylene blue which had been functionalised with a carboxylic acid group (using HSPyU) (Scheme 2 and Scheme S2, ESI†). The antimicrobial photodynamic therapy agent MB-PMX, was obtained after TFA deprotection of the Boc groups and HPLC purification (ESI†). The carboxylic acid derivative of methylene blue (MB-COOH) was prepared as previously reported[32] *via* reaction of *N*-methyl aniline and ethyl 4-bromobutyrate followed by hydrolysis. The product, *N*-methyl-*N*-(carboxypropyl)aniline, was treated with the 2-amino-5-(dimethylamino)phenylthio-sulfonic acid (prepared from 4-(*N*,*N*′-dimethyl)aniline) to give MB-COOH in moderate overall yield (~25%).

MB-PMX showed very similar absorption and emission features to that of unconjugated MB (Fig. 1a and b) with an absorption maxima at 670 nm with a weak emission centred around 694 nm upon excitation at 610 nm (10 μM in Saline (0.9% NaCl)). The robustness of MB-PMX (50 μM in 0.9% NaCl) was investigated with illumination at 630 nm, 10 mW cm^{-2} over 60 min and showed excellent photo-stability with its absorbance only decreasing by 10% during 60 min of irradiation. As expected, increasing the power to 40 mW cm^{-2} (for 60 min) resulted in more significant photo bleaching but still 60% of the probe survived (Fig. S3, ESI†).

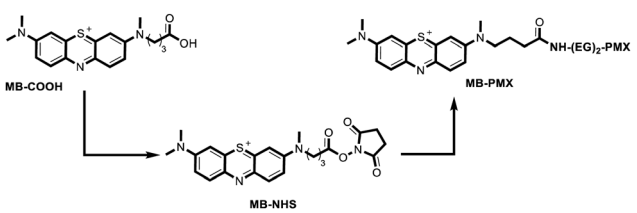

Scheme 2 Synthetic route to MB-PMX.

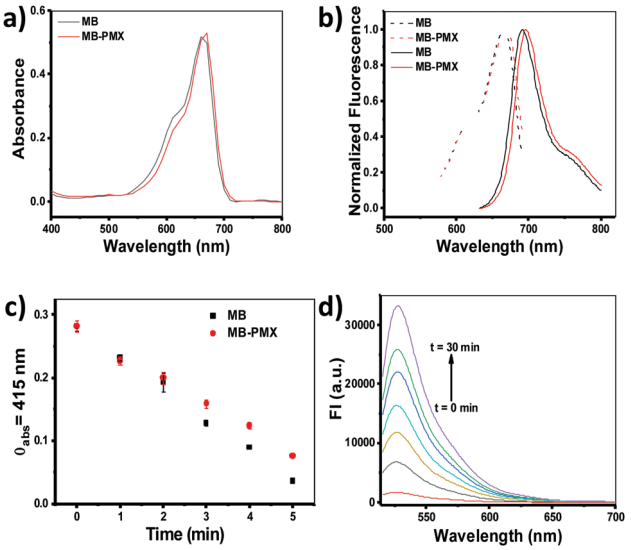

Fig. 1 (a) Absorbance spectra of MB and MB-PMX (10 μM in saline (0.9% NaCl)). (b) Excitation (dashed line) and emission (solid line) spectra of MB and MB-PMX (10 μM in saline (0.9% NaCl)). (c) Decrease in absorbance of the singlet oxygen trap (DPBF) at 415 nm (MB-PMX (5 μM) and DPBF (50 μM) in methanol, 630 nm, 1.5 mW cm^{-2}). (d) Increase in the fluorescence signal of ROS trap molecule DHR 123 (MB-PMX (10 μM) and DHR 123 (10 μM) in water at different time points (t = 0, 5, 10, 15, 20, 25, 30 min) 630 nm, 1.5 mW cm^{-2}) (λ_{exc} = 500 nm).

The singlet oxygen generation ability of MB-PMX was assessed using diphenylisobenzofuran (DPBF), which quickly traps singlet oxygen *via* endo-peroxide formation (that subsequently decomposes to 1,2-dibenzoylbenzene).[33] Mixtures of MB-PMX (5 μM) and DPBF (50 μM) were continuously irradiated and the decrease in absorbance measured at 415 nm (Fig. 1c). The absorbance band of DPBF disappeared within a few minutes with a measured singlet oxygen quantum yield of ϕ_Δ = 0.4 (using MB as the reference photosensitizer with ϕ_Δ = 0.5).[11] The ability of the probe to generate other reactive oxygen species (*i.e.* superoxide) *via* type I photo-process was explored using dihydrorhodamine 123 (DHR 123) (10 μM in water).[34] In this case the increase in fluorescence emission at 526 nm was monitored (λ_{ex} = 500 nm) and as shown in Fig. 1d increased with irradiation time, validating that MB-PMX produces both singlet oxygen and other ROS *via* type I and type II mechanisms.

The sensitivity, specificity and phototoxicity of MB-PMX was explored against a panel of pathogenic bacteria using Gram-negative *Escherichia coli* and *Pseudomonas aeruginosa*, with *Staphylococcus aureus* as a Gram-positive control. Unsurprisingly there was no reduction in CFU for any strain with just illumination (Fig. 2a and Fig. S6, ESI†), and for *S. aureus* there was no reduction under any condition, including MB-PMX plus illumination, indicating that MB-PMX was unable to bind to Gram-positive bacteria and elicit a phototoxic effect. With *E. coli* and *P. aeruginosa*, 100% killing (10^8 fold reduction in CFU mL^{-1}) was achieved following 10 min MB-PMX exposure and illumination (Fig. 2a and Fig. S6, ESI†). Transmission

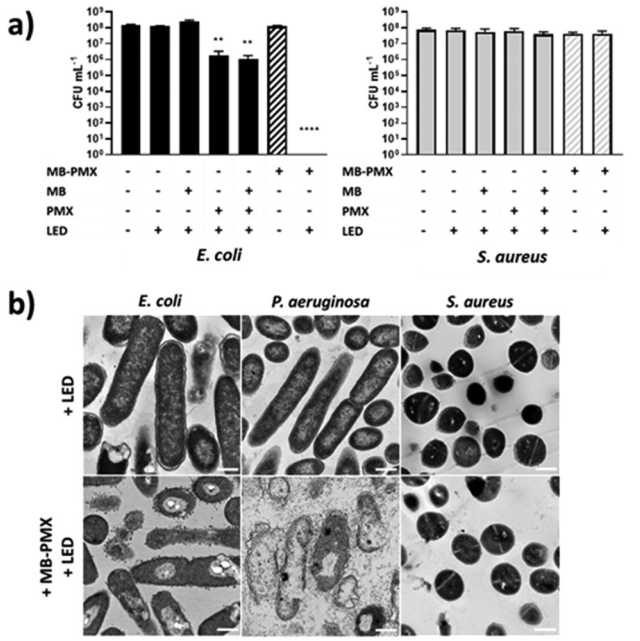

Fig. 2 (a) Colony forming units (CFU) of Gram-negative (black bars) and Gram-positive (grey bars) bacteria with 10 μM MB and/or 10 μM PMX-B (solid bars) or MB-PMX (10 μM, dashed bars), following 10 min illumination at 630 nm, 10 mW cm^{-2}. No illumination and/or no photosensitiser served as controls. Error bars show s.e.m., analysed by student *t*-test with comparison to bacteria-only control: ****$P < 0.0001$; **$P < 0.001$. $n \geq 3$ repeats. (b) Transmission electron microscopy (TEM) of *E. coli*, *P. aeruginosa* and *S. aureus* post PDT treatment with 10 μm MB-PMX and 10 min illumination at 630 nm, 10 mW cm^{-2}. Controls were irradiated without MB-PMX. Images captured with 12 000× magnification, scale bar = 500 nm.

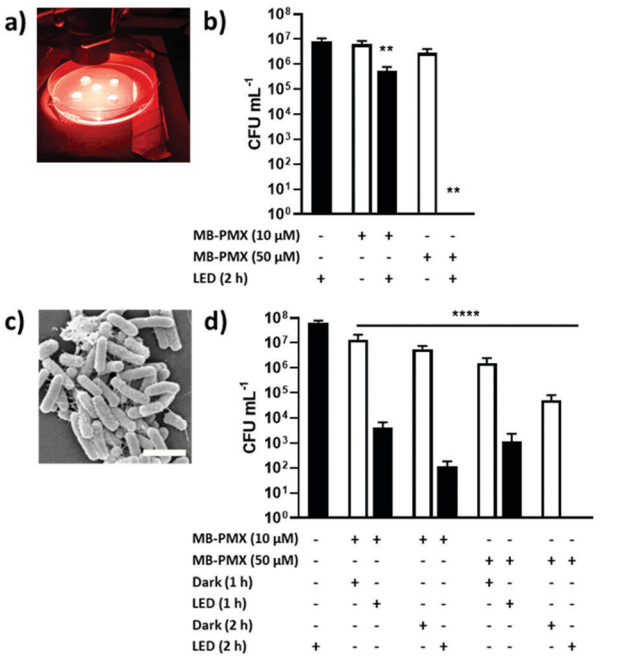

Fig. 3 (a) Image of infected porcine skin punches undergoing PDT. (b) Colony forming units (CFU) recovered from infected porcine skin post treatment with MB-PMX and illumination 630 nm, 40 mW cm^{-2} for 2 h. Error bars show s.e.m. Analysed by one-way ANOVA comparison to illumination only control: **$P = 0.0079$, **$P = 0.0046$. $n = 5$, performed in duplicate. (c) Representative SEM image of *E. coli* biofilms grown and treated by PDT with MB-PMX. Scale bar = 2 μm. (d) Colony forming units (CFU) recovered from *E. coli* biofilms following treatment with MB-PMX and illumination at 630 nm, 40 mW cm^{-2}. Analysed by one-way ANOVA comparison to bacteria-only control: ****$P < 0.0001$. $n = 3$, performed in duplicate.

electron microscopy (TEM) of the bacterial samples showed membrane disruption (blebbing) with a total breakdown of the bacterial cell wall following MB-PMX exposure and illumination (Fig. 2b). Whilst MB-PMX was able to perturb the cell membrane of Gram-negative bacteria following illumination, no disruption to the cell wall of *S. aureus* or haemolysis of human red blood cells was observed following equivalent illumination in the presence of excess MB-PMX, at concentrations of up to 10 fold of those used in our planktonic bacteria studies (Fig. 2b and Fig. S7, ESI†).

Compared to MB-PMX, the independent killing efficiency of MB and PMX-B was poor when added to the cultures together followed by irradiation. Indeed, there was no killing effect mediated by MB (10 μM) alone. PMX-B alone (10 μM) did exhibit bactericidal effect on planktonic *E. coli* and *P. aeruginosa* under the same conditions with a 10^2 fold reduction in CFU mL^{-1} for *E. coli*, and a 10^5 reduction in CFU mL^{-1} observed for *P. aeruginosa*. *P. aeruginosa* was also susceptible to MB-PMX without illumination, with a 10^3 fold reduction in CFU mL^{-1} measured, indicating that the polymyxin domain of our PDT agent was still active and potent. However, as demonstrated the MB-PMX conjugate with illumination gave complete microbial killing demonstrating excellent selectivity and sensitivity at low concentrations and was far superior to the MB plus PMX-B strategy (for further explanation see Fig. S6, ESI†).

Antimicrobial photodynamic therapy is an approach well suited to surface infections, such as those associated with the skin, or for the treatment of surfaces prior to surgical interventions such as orthopaedic implants. This has the added benefit of topical application of PDT photosensitizes mitigating against potential unwanted cytotoxic affects, often associated with systemic delivery of antimicrobials. To assess the feasibility of our antibacterial PDT approach, we utilised a porcine skin model of an early stage *E. coli* infection, similar to that utilised by Maisch *et al.*[35] and assessed the efficacy of MB-PMX (Fig. 3). Porcine skin samples were excised using a biopsy punch and stabilised within an agarose mount before being inoculated with *E. coli*. MB-PMX was added and the sample irradiated (Fig. 3a) (or maintained in the dark as a control). The tissue was homogenised, and bacterial levels quantified (Fig. 3b). MB-PMX in the dark did not elicit any antibacterial effect, however MB-PMX (10 μM) with illumination resulted in bacterial killing, eliciting an 11-fold reduction in bacterial count, whilst complete killing of the bacteria was observed with 50 μM MB-PMX treatment and 2 h illumination.

Early *E. coli* biofilms were established and their composition of bacteria (3D, non-motile aggregates and extracellular matrix deposition) confirmed by scanning electron microscopy (Fig. 3c and Fig. S8, ESI†). We observed complete killing of *E. coli* biofilms

with MB-PMX in a dose and time dependent manner, with a 10^8 reduction in CFU mL^{-1} achieved with 50 μM MB-PMX and 2 hours of illumination (630 nm, 40 mW cm^{-2}) (Fig. 3d). Even with as little as 10 μM MB-PMX and 1 h illumination, a 50% reduction in bacterial biofilm viability was achieved, demonstrating the potency of our Gram-negative specific PDT agent.

In conclusion, we have developed a novel antimicrobial photodynamic therapy agent, MB-PMX, which demonstrates selective and potent photodynamic bactericidal activity against Gram-negative bacteria, with efficacy against clinical isolates of *E. coli* and *P. aeruginosa*. Not only did MB-PMX show outstanding antimicrobial PDT activity against planktonic bacteria with 100% pathogen killing with short light irradiation times but it also demonstrated the ability to treat biofilms and infected skin models, whilst having no effect on Gram-positive *S. aureus* or human erythrocytes. Here we have demonstrated potency against early, mono-species biofilms and infections, and thus further evaluation of complex multispecies biofilm and skin wounds is warranted to further elucidate the potential role of PDT with MB-PMX as an alternative to antimicrobial treatments. The targeting effect of the polymyxin ligand ensures that the killing functionality of the reactive oxygen species is not only highly localised (where it can induce the most damage), but is also concentrated on the target itself – leading to much higher therapeutic efficacies.

We thank the Engineering and Physical Sciences Research Council (grants EP/K03197X/1 and EP/R005257/1); and the Wellcome Trust Multi User Equipment Grant (WT104915MA) for use of the TEM and SEM microscopes, and the CALM imaging facilities at the Queens Medical Research Institute, University of Edinburgh.

Conflicts of interest

There are no conflicts to declare.

Notes and references

1 B. Spellberg, R. Guidos, D. Gilbert, J. Bradley, H. W. Boucher, W. M. Scheld, J. G. Bartlett and J. Edwards, Jr., A. Infectious Diseases Society of, *Clin. Infect. Dis.*, 2008, **46**, 155–164.
2 M. M. D. Pinky Sarmah, D. Adapa and T. K. Sarangi, *Electronic J. Biol.*, 2018, **14**, 50–58.
3 T. T. Yoshikawa, *J. Am. Geriatr. Soc.*, 2002, **50**, 226–229.
4 R. I. Aminov, *Front. Microbiol.*, 2010, **1**, 134.
5 C. L. Ventola, *P & T*, 2015, **40**, 277–283.
6 H. X. Zheng Huang, A. D. Meyers, A. I. Musani, L. Wang, R. Tagg, Al B. Barqawi and Y. K. Chen, *Technol. Cancer Res. Treat.*, 2008, **7**, 309–320.
7 M. Tampa, M. I. Sarbu, C. Matei, C. I. Mitran, M. I. Mitran, C. Caruntu, C. Constantin, M. Neagu and S. R. Georgescu, *Oncol. Lett.*, 2019, **17**, 4085–4093.
8 Y. K. Tandon, M. F. Yang and E. D. Baron, *Photodermatol., Photoimmunol. Photomed.*, 2008, **24**, 222–230.
9 G. Plotino, N. M. Grande and M. Mercade, *Int. Endod. J.*, 2019, **52**, 760–774.
10 A. A. Foggiato, D. F. Silva and R. Castro, *Photodiagn. Photodyn. Ther.*, 2018, **24**, 123–128.
11 R. J. C. Maria and C. DeRosa, *Coord. Chem. Rev.*, 2002, **233-234**, 251–271.
12 M. Wainwright, T. Maisch, S. Nonell, K. Plaetzer, A. Almeida, G. P. Tegos and M. R. Hamblin, *Lancet Infect. Dis.*, 2017, **17**, e49–e55.
13 F. Cieplik, L. Tabenski, W. Buchalla and T. Maisch, *Front. Microbiol.*, 2014, **5**, 405.
14 F. Cieplik, D. Deng, W. Crielaard, W. Buchalla, E. Hellwig, A. Al-Ahmad and T. Maisch, *Crit. Rev. Microbiol.*, 2018, **44**, 571–589.
15 T. Dai, Y. Y. Huang and M. R. Hamblin, *Photodiagn. Photodyn. Ther.*, 2009, **6**, 170–188.
16 S. Morley, J. Griffiths, G. Philips, H. Moseley, C. O'Grady, K. Mellish, C. L. Lankester, B. Faris, R. J. Young, S. B. Brown and L. E. Rhodes, *Br. J. Dermatol.*, 2013, **168**, 617–624.
17 J. P. Tardivo, F. Adami, J. A. Correa, M. A. Pinhal and M. S. Baptista, *Photodiagn. Photodyn. Ther.*, 2014, **11**, 342–350.
18 X. Lei, B. Liu, Z. Huang and J. Wu, *Arch. Dermatol. Res.*, 2015, **307**, 49–55.
19 M. L. Embleton, *J. Antimicrob. Chemother.*, 2002, **50**, 857–864.
20 R. Dosselli, M. Gobbo, E. Bolognini, S. Campestrini and E. Reddi, *ACS Med. Chem. Lett.*, 2010, **1**, 35–38.
21 R. Cahan, N. Swissa, G. Gellerman and Y. Nitzan, *Photochem. Photobiol.*, 2010, **86**, 418–425.
22 D. R. Rice, H. Gan and B. D. Smith, *Photochem. Photobiol. Sci.*, 2015, **14**, 1271–1281.
23 F. S. Felipe, H. Ying-Ying and R. H. Michael, *Recent Pat. Anti-Cancer Drug Discovery*, 2013, **8**, 108–120.
24 M. Jamal, W. Ahmad, S. Andleeb, F. Jalil, M. Imran, M. A. Nawaz, T. Hussain, M. Ali, M. Rafiq and M. A. Kamil, *J. Chin. Med. Assoc.*, 2018, **81**, 7–11.
25 M. E. Olson, H. Ceri, D. W. Morck, A. G. Buret and R. R. Read, *Can. J. Vet. Res.*, 2002, **66**, 86–92.
26 F. Rabanal and Y. Cajal, *Nat. Prod. Rep.*, 2017, **34**, 886–908.
27 Y. Nitzan, M. Gutterman, Z. Malik and B. Ehrenberg, *Photochem. Photobiol.*, 1992, **55**, 89–96.
28 F. Le Guern, V. Sol, C. Ouk, P. Arnoux, C. Frochot and T. S. Ouk, *Bioconjugate Chem.*, 2017, **28**, 2493–2506.
29 F. Le Guern, T. S. Ouk, C. Ouk, R. Vanderesse, Y. Champavier, E. Pinault and V. Sol, *ACS Med. Chem. Lett.*, 2018, **9**, 11–16.
30 T. T. Vy Phan, S. Bharathiraja, V. T. Nguyen, M. S. Moorthy, P. Manivasagan, K. D. Lee and J. Oh, *RSC Adv.*, 2017, **7**, 35027–35037.
31 A. R. Akram, S. V. Chankeshwara, E. Scholefield, T. Aslam, N. McDonald, A. Megia-Fernandez, A. Marshall, B. Mills, N. Avlonitis, T. H. Craven, A. M. Smyth, D. S. Collie, C. Gray, N. Hirani, A. T. Hill, J. R. Govan, T. Walsh, C. Haslett, M. Bradley and K. Dhaliwal, *Sci. Transl. Med.*, 2018, **10**, eaal0033.
32 E. Gonzalez-Fernandez, N. Avlonitis, A. F. Murray, A. R. Mount and M. Bradley, *Biosens. Bioelectron.*, 2016, **84**, 82–88.
33 M. Ucuncu, E. Karakus, E. Kurulgan Demirci, M. Sayar, S. Dartar and M. Emrullahoglu, *Org. Lett.*, 2017, **19**, 2522–2525.
34 M. Li, T. Xiong, J. Du, R. Tian, M. Xiao, L. Guo, S. Long, J. Fan, W. Sun, K. Shao, X. Song, J. W. Foley and X. Peng, *J. Am. Chem. Soc.*, 2019, **141**, 2695–2702.
35 T. Maisch, C. Bosl, R. M. Szeimies, B. Love and C. Abels, *Photochem. Photobiol. Sci.*, 2007, **6**, 545–551.

